

QForte: an efficient state simulator and quantum algorithms library for molecular electronic structure

Nicholas H. Stair and Francesco A. Evangelista*

Department of Chemistry and Cherry Emerson Center for Scientific Computation, Emory University, Atlanta, Georgia, 30322, U.S.A.

E-mail: francesco.evangelista@emory.edu

Abstract

We introduce a novel open-source software package QForte, a comprehensive development tool for new quantum simulation algorithms. QForte incorporates functionality for handling molecular Hamiltonians, fermionic encoding, ansatz construction, time evolution, and state-vector simulation, requiring only a classical electronic structure package as a dependency. QForte also contains black-box implementations of a wide variety of quantum algorithms including (but not limited to): variational and projective quantum eigensolvers, adaptive eigensolvers, quantum imaginary time evolution, quantum Krylov methods, and quantum phase estimation. We highlight two features of QForte: i) how the Python class structure of QForte enables the facile implementation of new algorithms, and ii) how existing algorithms can be executed in just a few lines of code.

1. INTRODUCTION

The past decade has seen tremendous progress in the development of quantum computational hardware, enabling early demonstrations of quantum advantage,¹ and numerous non-trivial applications ranging from quantum simulation²⁻⁷ to constrained optimization.^{8,9} These advances have concurrently inspired rapid development of numerous quantum algorithms amenable to both noisy intermediate-scale quantum¹⁰ (NISQ) and fault-tolerant devices. In the field of quantum simulation of many-body systems, a variety of methods now exist¹¹⁻¹⁵ which vary dramatically in quantum resource requirements, often with a tradeoff between circuit depth and measurement overhead. Unfortunately, new quantum algorithmic developments are rarely accompanied by detailed numerical comparison to existing algorithms. The infrequency of cross comparison is largely due to the lack of widely accessible reference implementations of new quantum algorithms. To help ameliorate this issue, we introduce a new open-source software project, QForte, the first black-box quantum algorithms library for molecular electronic structure.

The software ecosystem for the development of new quantum algorithms is ever-expanding, ranging from full-stack industry backed packages,¹⁶⁻²⁰ to task specific open source projects.²¹⁻²⁸ This is particularly true in the context of quantum algorithms for molecular electronic structure, because there are many complex software challenges involved in the complete user workflow pipeline illustrated in Fig. 1, beginning with specification of a molecular geometry and ending with a numerical prediction of the molecular energy (and properties). In order to accomplish this task, one must use a classical electronic structure package (e.g., PySCF,²⁹ Psi4,³⁰ etc.) to obtain the matrix representation of one- (h_{pq}) and

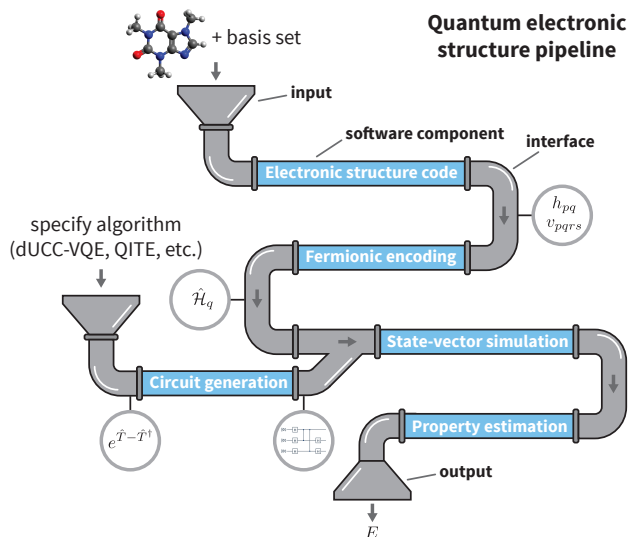


Figure 1: The quantum electronic structure pipeline.

two-body (v_{pqrs}) operators (integrals) that define the molecular Hamiltonian

$$\hat{\mathcal{H}} = \sum_{pq} h_{pq} \hat{a}_p^\dagger \hat{a}_q + \frac{1}{4} \sum_{pqrs} v_{pqrs} \hat{a}_p^\dagger \hat{a}_q^\dagger \hat{a}_s \hat{a}_r \quad (1)$$

where \hat{a}^\dagger and \hat{a} are, respectively, fermionic creation and annihilation operators labeled by the index of the spin orbital on which they act. Next, one must utilize a package for fermionic encoding (e.g., OPENFERMION), as well as appropriate application programming interfaces (API) (e.g., OPENFERMION-PYSCF or OPENFERMION-Psi4), to map fermionic operators

(such as the Hamiltonian, $\hat{\mathcal{H}}$) to the so-called qubit representation ($\hat{\mathcal{H}}_q$) given as a linear combination of a given number (N_{PS}) of Pauli strings (products of Pauli operators) \hat{P}_ℓ :

$$\hat{\mathcal{H}} \xrightarrow{\text{fermionic encoding}} \hat{\mathcal{H}}_q = \sum_{\ell}^{N_{\text{PS}}} h_{\ell} \hat{P}_{\ell} \quad (2)$$

In order to apply quantum circuits associated with encoded operators (such as the time evolution unitary, or various unitary ansätze) one is required to install one of the numerous backend quantum-computer simulators such as those implemented in QISKIT¹⁶ (IBM), CIRQ¹⁷ and FQE²¹ (Google), Q#¹⁸ (Microsoft), or PYQUILL¹⁹ (Rigetti), each associated with a distinct API.

In the outermost software layer exist packages such as TEQUILA²⁶ that serve as sandbox implantation tools which solve many of the interoperability challenges associated with interfacing the aforementioned dependencies. While flexible packages for sand-box development are undoubtedly important, it is still usually left to the user to implement a desired algorithm, which is generally a non-trivial task given the diversity of quantum algorithms present in modern literature and the challenge of utilizing an inhomogeneous software ecosystem. A single-package (incorporating all of the described steps) black-box implementation of quantum algorithms with which one can easily specify a molecular geometry and desired quantum algorithm (as is the case for classical electronic structure packages) is highly desirable for researchers interested in generating comparative results rapidly.

An additional challenge to black-box implementation of quantum algorithms is their now significant level of diversity. Arguably the simplest and most well established (hybrid) algorithm is the variational quantum eigensolver^{11,12} (VQE). In VQE, the ground state is approximated by a trial state optimized in a procedure that combines a classical optimization algorithm with quantum measurement of the energy and gradients of the trial state. While implementation of a vanilla VQE code is straightforward for toy examples, automatic generation of the ansatz circuit is generally more complicated and obviously dependent on the specific form of the ansatz (i.e. disentangled unitary coupled cluster,^{12,31,32} hardware-efficient,³ Hamiltonian variational,³³ qubit coupled cluster,³⁴ to name a few). Moreover, many hybrid approaches such as adaptive ansatz approaches^{35,36} or subspace expansion methods³⁷ incorporate the basic VQE schema as a subroutine and require additional implementation for determination of matrix elements to solve a generalized eigenvalue problem and/or an additional algorithmic layer to extend the ansatz. Similar implementation challenges exist for algorithms that rely on (often controlled) Hamiltonian time evolution such as quantum phase estimation³⁸⁻⁴⁰ (QPE), or time-evolved subspace methods.⁴¹⁻⁴³ For algorithms that measure projected quantities such as quantum imaginary time evolution¹³ (QITE) and the projective quantum eigensolver⁴⁴ (PQE), one must additionally implement the (often iterative) parameter update procedure.

Our new open-source package QFORTE is an end-to-end

electronic structure package for quantum algorithms, and is still capable of facilitating sand-box implementations of new algorithms, only relying on a classical electronic structure package as a dependency. The remainder of this article is organized as follows. In Sec. 2 we will describe key component classes in QFORTE and its interface to Psi4. In Sec. 3 will discuss each of the quantum algorithms currently implemented in QFORTE as well as some of their implementation details in terms of the key components. In Sec. 4 we discuss representative timings for critical subroutines such as determining Hamiltonian expectation values. Finally, in Sec. 5 we demonstrate an example of how QFORTE can (i) be used to implement a new quantum algorithm and (ii) be used to compare new algorithms to the ones already implemented in its library.

2. OVERVIEW OF THE STRUCTURE OF QFORTE

In order to facilitate simple molecular-geometry to quantum algorithm energy functionality, QFORTE wraps the entire quantum electronic structure pipeline in a black-box code. The main software components of QFORTE are illustrated in Fig. 2. The lowest level contains components that require efficient execution, including the state-vector simulator (Computer) and quantum circuits (Circuit). These are implemented as classes in C++ and exposed in Python via PYBIND11.⁴⁵ Higher-level components such as the SystemFactory class which interfaces QFORTE to classical electronic structure packages, and the subclasses that implement algorithms are all written in Python and use the PYBIND11 interface to the lower-level components. Here we will give an overview of some of the most important components of QFORTE.

2.1 The state-vector simulator. An important aspect of QFORTE that distinguishes it from many other packages is its incorporation of a dedicated state-vector simulator. State-vector simulators store and manipulate a classical representation of the full quantum state that exists on quantum hardware.

The QubitBasis class. The state-vector simulator in QFORTE makes heavy use of an elementary C++ QubitBasis class used to represent an element of a n_{qb} qubit Fock space basis $\mathcal{F} = \{|q_0\rangle \otimes \cdots \otimes |q_{n_{\text{qb}}-1}\rangle\}$. Each instance of QubitBasis represents an element of \mathcal{F} , and is characterized by a 64-bit unsigned integer such that each bit represents the binary state of a qubit:

$$\underbrace{q_{63} \cdots q_1 q_0}_{\text{64-bit unsigned integer}} \equiv \underbrace{|q_0\rangle \otimes \cdots \otimes |q_{63}\rangle}_{\text{element of the Fock-space basis}}, \quad \text{with } q_i \in \{0, 1\} \quad (3)$$

Because application of quantum gates to any basis element results in flipping the state of target qubit(s), use of the unsigned integer type is beneficial as it allows for very efficient bitwise operations. The binary number corresponding to an element of the Fock-space basis also offers a convenient way to map the qubit multi-index $q_0 q_1 \cdots$ to a single index (address).

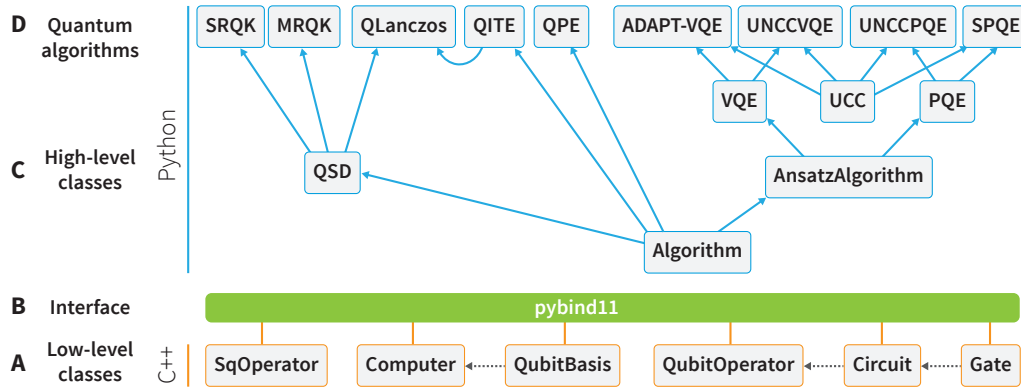


Figure 2: The structure of the QFortE package. Solid lines indicate inheritance (pointing from the base to the derived class) while dashed lines indicate use of objects from another class (pointing from the class used to the one using it). A) Low-level C++ classes are used to store and manipulate a state vector. B) The C++ classes are exposed to Python via the `pybind11` library. C) A high-level Python classes implement components of quantum algorithms. D) Quantum algorithms available to the user are implemented using classes from the high-level API.

The QuantumComputer class. The backbone of the state-vector simulator in QFORTE is the `Computer` class, which, for a given number of qubits (n_{qb}) stores a state vector of the form

$$|\Psi_q\rangle = \sum_{q_0 \dots q_{n_{\text{qb}}-1}}^{\{0,1\}} C_{q_0, \dots, q_{n_{\text{qb}}-1}} |q_0\rangle \otimes \dots \otimes |q_{n_{\text{qb}}-1}\rangle \quad (4)$$

By default, a `Computer` object is initialized in the state $|\Psi_q\rangle = |0\rangle \otimes \dots \otimes |0\rangle$. The `Computer` class is comprised of a complex vector to store $C_{q_0, \dots, q_{n_{\text{qb}}-1}}$, as well as a vector of `QubitBasis` objects (both of dimension $2^{n_{\text{qb}}}$ where n_{qb} is the number of qubits). An example of how to instantiate a `Computer` with four qubits is shown in Lst. 1.

```
1 import qforte as qf
2 nqb = 4
3 qcomp = qf.Computer(nqb)
```

Listing 1: Initializing a `Computer` object with four qubits.

The Gate class. Once a `Computer` is initialized, the state can be modified by applying gates, encoded in the class `Gate`. The `Gate` class (when used in conjunction with a `Computer`) is the most fundamental building block for all quantum algorithms in QFORTE. Some of the most pertinent gates used in quantum simulation are the Pauli gates (X , Y , and Z), the Hadamard gate H (not to be confused with the Hamiltonian \hat{H}), the controlled NOT [CNOT] gate, and the parametric z rotation gate $R_z(\theta)$. A full list of gates implemented in QFORTE can be found in the documentation.

The `Gate` class has several important attributes including its type, the target (and optionally the control) qubit index, and a matrix of complex values that represents the operator. Instantiating a `Gate` is simply done via the `gate()` member function, as shown in Lst. 2.

```
1 target_idx = 4
```

```
2 X_4gate = qf.gate('X', target_idx)
```

Listing 2: Initializing a `Gate` object. Here we instantiate a Pauli X gate that will target the qubit q_4 .

Listing 3 shows a small example of using QFORTE’s state-vector simulator to construct the two-qubit Bell state

$$|\Psi_{\text{Bell}}\rangle = \frac{1}{\sqrt{2}} |00\rangle + \frac{1}{\sqrt{2}} |11\rangle \quad (5)$$

by applying H_0 followed by $\text{CNOT}_{0,1}$ to the state $|00\rangle$. Recall that the action of the Hadamard gate H is:

$$H|0\rangle = \frac{1}{\sqrt{2}}(|0\rangle + |1\rangle), \quad H|1\rangle = \frac{1}{\sqrt{2}}(|0\rangle - |1\rangle) \quad (6)$$

Recall that the action of the controlled NOT gate [with target qubit q_0 , and control qubit q_1 ($\text{CNOT}_{0,1}$)] is:

$$\begin{aligned} \text{CNOT}_{0,1} |00\rangle &= |00\rangle & \text{CNOT}_{0,1} |01\rangle &= |11\rangle \\ \text{CNOT}_{0,1} |10\rangle &= |10\rangle & \text{CNOT}_{0,1} |11\rangle &= |01\rangle \end{aligned} \quad (7)$$

```
1 # Initialize a two-qubit QuantumComputer.
2 nqb = 2
3 qbell = qf.Computer(nqb)
4
5 # Initialize the gates needed to build the
6 # Bell state.
7 H_0 = qf.gate('H', 0)
8 CNOT_0_1 = qf.gate('CNOT', 1, 0)
9
10 # Apply the Hadamard gate.
11 qbell.apply_gate(H_0)
12
13 # Apply the CNOT gate.
14 qbell.apply_gate(CNOT_0_1)
```

Listing 3: Creating a Bell state using a circuit that applies the unitary $\text{CNOT}_{0,1}H_0$ to the state $|00\rangle$.

In QFORTE, the action of a gate on a quantum state (represented by a `Computer` object) is implemented with efficient

algorithms specialized for different gates. For example, in Fig. 3 we illustrate how the X_2 operator is applied to a 3-qubit state. Since X_2 modifies only the first bit (by flipping it), the operation $X_2 |\Psi\rangle \rightarrow |\Psi'\rangle$ can be efficiently implemented with a low-level copy operation that realizes the following action on the coefficients in a `Computer` object: $C'_{q_0 q_1 q_2} = C_{q_0 q_1 (1-q_2)}$. Since the operation is performed on continuous sections of the state vector, the effect of cache misses is minimized and the operation can be easily vectorized on multi-core architectures. The same principle illustrated here can be applied to more complex one-qubit gates such as parameterized rotations and two-qubit gates such as CNOT.

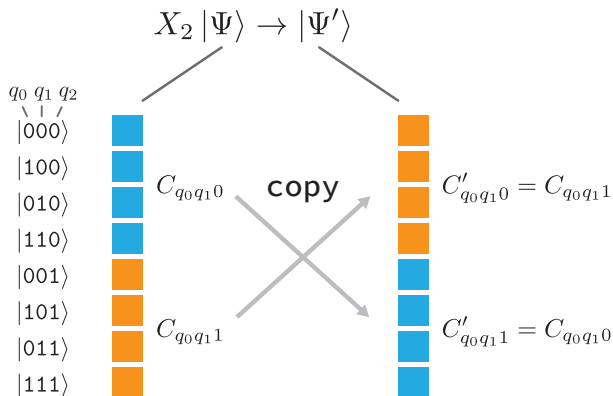


Figure 3: Example of how gate operations are implemented in QFORTE. In this example, the X_2 gate is applied to a general state Ψ producing a new state Ψ' . The action of X_2 can be implemented efficiently with a low-level C++ copy operation to two separate portions of the state vector.

The Circuit class. In virtually any quantum algorithm it is necessary to apply many gates sequentially. A so-called quantum circuit, commonly referred to as a unitary (\hat{U}), is represented by a product of quantum gates, making the overall circuit itself a unitary operation. The `Circuit` class operates at one level above the `Gate` class and its primary attribute is a vector of `Gate` objects.

Although any product of elementary gates technically constitutes a circuit, one of the most important circuit structures in quantum simulation is that which represents unitaries obtained by exponentiating a product of Pauli operators:

$$e^{i\theta_\ell \hat{P}_\ell} \quad (8)$$

where

$$\hat{P}_\ell = \prod_k^{n_\ell} \hat{\sigma}_k^{(\ell)} \quad (9)$$

is a unique product of n_ℓ Pauli operators $\hat{\sigma}_k^{(\ell)}$. The compound index $k = (p, [X, Y, \text{ or } Z])$ labels a combination of a specific Pauli operator and the qubit (p) on which it acts. The function `exponentiate_pauli_string` in QFORTE is responsible for converting Eq. (8) into a circuit containing one- and two-qubit gates. An example of how one would construct such a circuit in QFORTE for the operator

$\exp(-i0.5 X_2 Z_1 Z_0)$ is shown in Lst. 4, while in Fig. 4 we report the corresponding quantum circuit generated by the function `exponentiate_pauli_string`. This algorithm follows a standard approach^{11,12,46} of using operator identities (e.g., like $X = HZH$) to express the starting expression in terms of the exponential of products of Z operators only, namely

$$\begin{aligned} \exp(-i0.5 X_2 Z_1 Z_0) &= \exp(-i0.5 H_2 Z_2 H_2 Z_1 Z_0) \\ &= H_2 \exp(-i0.5 Z_2 Z_1 Z_0) H_2 \end{aligned} \quad (10)$$

where one uses the fact that H_2 is its own inverse ($H_2 H_2 = 1$) and that it commutes with Z_0 and Z_1 . Next, the term $\exp(-i0.5 Z_2 Z_1 Z_0)$, responsible for the fermionic sign, is implemented as a cascade of CNOT gates, a z-axis rotation of $2\theta_\ell$, and the inverse of the CNOT cascade:

$$e^{-i0.5 Z_2 Z_1 Z_0} = \text{CNOT}_{0,1} \text{CNOT}_{1,2} R_z(1.0) \text{CNOT}_{1,2} \text{CNOT}_{0,1} \quad (11)$$

```

1 # Construct the desired preliminary circuit
  (X2 Z1 Z0)
2 circ = qf.Circuit()
3 circ.add_gate(qf.gate('Z', 0))
4 circ.add_gate(qf.gate('Z', 1))
5 circ.add_gate(qf.gate('X', 2))
6
7 # Define the factor = -i theta
8 factor = -0.5j
9
10 # Construct the unitary for the exponential.
11 Uexp, phase = exponentiate_pauli_string(
    factor, circ)

```

Listing 4: Constructing the circuit corresponding to the operator $\exp(-i0.5 X_2 Z_1 Z_0)$.

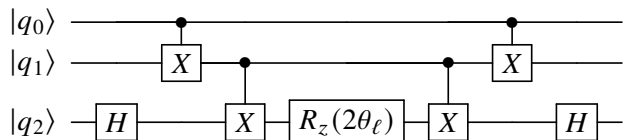


Figure 4: Circuit diagram for exponential unitary operators commonly used in many quantum simulation algorithms. This example considers operators of the form $\exp(-i\theta_\ell X_2 Z_1 Z_0)$.

2.2 The QubitOperator and SQOperator classes. The outer-most operations class in QFORTE is the `QubitOperator` class. This class represents operators \hat{O} that are linear combinations of N_ℓ unitaries (\hat{U}_ℓ) as

$$\hat{O} = \sum_\ell u_\ell \hat{U}_\ell \quad (12)$$

where u_ℓ is a complex coefficient. The key attribute of the `QubitOperator` class is a vector of pairs containing a complex coefficient and a `Circuit` object. In QFORTE's implementation, the `QubitOperator` class is used to represent

objects such as the Hamiltonian $\hat{\mathcal{H}}_q$ or the cluster operator⁴⁷ \hat{T}_q (in their qubit representations). It is important to note that although it is always possible in QFORTE to apply a `QubitOperator` to a state, unless \hat{O} is unitary, this operation cannot be realized physically on a quantum device.

The ability to evaluate expectation values of the form $\langle \hat{O} \rangle = \langle \Psi_q | \hat{O} | \Psi_q \rangle$ is also paramount to many quantum algorithms. Examples include the energy and energy gradients for VQE, as well as projected quantities such as off-diagonal matrix elements in QSD techniques, or residuals in PQE. In QFORTE this is accomplished easily by passing the operator to an exception value function. Listing 5 for example shows how one would measure the expectation value of the operator $\hat{O} = X_0 + \hat{X}_1$ with respect to the Bell state (constructed in Lst. 3). We note that it is also possible to determine approximate expectation values in QFORTE based on a user specified number of measurements.

```

1 # Initialize the operator
2 O = QubitOperator()
3 O.add_term(1.0, build_circuit('X_0'))
4 O.add_term(1.0, build_circuit('X_1'))
5
6 # Get the expectation value.
7 exp_val = qbell.direct_op_exp_val(O)

```

Listing 5: Measuring expectation values for `QubitOperators`.

QFORTE also supports operators in the form of second quantization, that is, operators comprised of fermionic annihilation and creation operators. The `SQOperator` class functions very similarly to the `QubitOperator` class, but utilizes a slightly different syntax. We note that second quantized operators in QFORTE always assume that the individual fermionic operators are normal ordered (creation operators appear to the left of annihilation operators) within a term. The second quantized operators can then be transformed to the `QubitOperator` representation (given as a linear combination of products of Pauli operators) via the Jordan-Wigner (JW) transformation.⁴⁸ Other common fermionic encodings⁴⁹⁻⁵² are not implemented natively in QFORTE and will be added in future releases. Under the JW transformation, there is a one-to-one mapping between a spin orbital ϕ_p and qubit q_p such that the fermionic annihilation (\hat{a}_p) and creation (\hat{a}_p^\dagger) operators are represented by combinations of Pauli strings

$$\hat{a}_p = \frac{1}{2}(X_p + iY_p)Z_{p-1} \dots Z_0 \quad (13)$$

and,

$$\hat{a}_p^\dagger = \frac{1}{2}(X_p - iY_p)Z_{p-1} \dots Z_0 \quad (14)$$

Listing 6 shows how to instantiate a `SQOperator` with the operator $0.5 \hat{a}_1^\dagger \hat{a}_2 - 0.25 \hat{a}_4^\dagger \hat{a}_2^\dagger \hat{a}_3 \hat{a}_1$ and transform it into a `QubitOperator`.

```

1 # Initialize the second quantized operator.
2 sq_op = qf.SQOperator()
3
4 # Construct the terms and add them to the
  list.
5 h1 = 0.5

```

```

6 h2 = -0.25j
7 sq_op.add_term(h1, [1], [2])
8 sq_op.add_term(h2, [4, 2], [3, 1])
9
10 # Transform to the qubit operator
   representation.
11 pauli_op = sq_op.jw_transform()

```

Listing 6: Converting `SQOperators` into `QuantumOperators`. This example constructs the operator $0.5 \hat{a}_1^\dagger \hat{a}_2 - 0.25 \hat{a}_4^\dagger \hat{a}_2^\dagger \hat{a}_3 \hat{a}_1$.

2.3 The molecule class. As discussed in the introduction, the first step in a quantum electronic structure computation is to obtain the molecular Hamiltonian in the qubit operator representation, based on a specified molecular geometry. In QFORTE this is all accomplished using the `system_factory` and `molecule` classes. To begin, as shown in Lst. 7, one simply imports the appropriate modules and specifies a geometry (in this case as a list of element symbols and xyz coordinates). Once the molecule class has been populated, the user has access to the molecular Hamiltonian both in its second-quantization representation (as a `SQOperator`) and in a qubit representation (as a `QubitOperator`) resulting from the Jordan-Wigner transformation. The molecule object is a key data structure in QFORTE that is passed to all algorithms to perform a quantum computation.

```

1 from qforte import *
2
3 # Define the molecular geometry.
4 geom = [('H', (0., 0., 0.)), ('H', (0., 0.,
   0.75))]
5
6 # Instantiate the system_factory object (
   also populates the integrals).
7 factory = system_factory(build_type='psi4',
   mol_geometry=geom, basis='sto-3g')
8
9 # Get the molecule object.
10 H2mol = factory.get_molecule()

```

Listing 7: Initializing the QFORTE molecule object.

3. ALGORITHMS IMPLEMENTED IN QFORTE

Quantum algorithms are implemented in QFORTE in the Python layer, and are built by composing abstract base classes (ABCs) that implement algorithms (and optionally) mixin classes that encode specific ansätze. For example, the lowest-level ABC in QFORTE is `Algorithm`, which is responsible for defining attributes and abstract functions common to all derived classes. The class `AnsatzAlgorithm`, derived from `Algorithm`, defines additional functionality that builds a quantum circuit for any algorithm that employs a parameterized ansatz. Each distinct algorithm implemented in QFORTE is then defined by its own concrete class that inherits from various appropriate parent classes, as displayed in Fig. 2.

We consider the algorithms implemented in QFORTE partitioned into several overlapping categories. The first is variational hybrid algorithms^{11,12,53} in which a classical optimizer is utilized to minimize the energy expectation value. The second category is projective approaches^{13,44} where projective quantities are measured on a quantum device and then

used to directly update or augment a classically parameterized unitary. The third category is quantum subspace diagonalization^{13,37,41,42,54} (QSD) in which a non-orthogonal many body basis is generated from a family of operators, and the matrix elements of a generalized eigenvalue problem are measured on a quantum device. Finally, there are those algorithms derived from quantum phase estimation^{39,40} where the eigenvalue of a time evolved state is estimated by a binary readout of a set of ancilla qubits.

Currently, QFORTE contains black-box implementations of the following algorithms: (i) variational quantum eigensolver^{11,12} (VQE) and (ii) projective quantum eigensolver⁴⁴ (PQE) both with a disentangled⁵⁵ (factorized) unitary coupled cluster^{56–60} (dUCC) ansatz, (iii) the adaptive derivative-assembled pseudo-trotter (ADAPT)-VQE,³⁵ (iv) selected PQE⁴⁴ (SPQE), (v) a variant of quantum imaginary time evolution¹³ (QITE) and its quantum Lanczos¹³ (QLanczos) extension, (vi) quantum Krylov^{41,42} (QK) and (vii) its selected multireference variant⁴² (MRSQK), and a pilot implementation of (vii) quantum phase estimation^{39,40} (QPE). Each of these algorithms is implemented using the software components described in Sec. 2. In the following subsections we will briefly summarize each of these methodologies.

3.1 Variational quantum eigensolver (VQE) based on dUCC trial states. In the general VQE schema, one uses a unitary circuit $\hat{U}(\theta)$ parameterized by the vector θ to construct a normalized trial state of the form

$$|\Psi_{\text{VQE}}\rangle = \hat{U}(\theta) |\Phi_0\rangle \quad (15)$$

from an easily prepared reference state $|\Phi_0\rangle$ (such as the Hartree–Fock state). One then minimizes the energy expectation value of the trial state

$$E(\theta) = \langle \Phi | \hat{U}^\dagger(\theta) \hat{H} \hat{U}(\theta) | \Phi \rangle \quad (16)$$

This minimization problem is solved by a classical optimization algorithm that calls a quantum routine to access the energy (and optionally gradients^{61,62}) of the trial state. Energy and gradients may be computed by averaging the expectation value of each term in the qubit Hamiltonian [Eq. (2)], for example

$$E(\theta) = \sum_t h_t \langle \Phi | \hat{U}^\dagger(\theta) \hat{P}_t \hat{U}(\theta) | \Phi \rangle \quad (17)$$

In QFORTE we have implemented VQE with a disentangled (or factorized) UCC ansatz $\hat{U}_{\text{dUCC}}(\mathbf{t})$. We assume a single determinant reference state $|\Phi_0\rangle = |\phi_1 \phi_2 \dots\rangle$ specified by occupied spin orbitals $\{\phi_i\}$ and unoccupied (virtual) spin orbitals $\{\phi_a\}$. The operator $\hat{\tau}_\mu \equiv \hat{\tau}_{ij\dots}^{ab\dots} = \hat{a}_a^\dagger \hat{a}_b^\dagger \dots \hat{a}_j \hat{a}_i$ is a particle-hole excitation operator that transforms the reference determinant $|\Phi_0\rangle$ into the excited determinant $|\Phi_\mu\rangle = \hat{\tau}_\mu |\Phi_0\rangle$. The dUCC ansatz is then constructed as a product of exponentiated anti-hermitian operators $\hat{\kappa}_\mu \equiv \hat{\tau}_\mu - \hat{\tau}_\mu^\dagger$ as

$$\hat{U}_{\text{dUCC}}(\mathbf{t}) = \prod_\mu e^{t_\mu \hat{\kappa}_\mu} \quad (18)$$

The dUCC circuit is built automatically in QFORTE by initial-

izing a SQOperator list that represent the $\hat{\kappa}_\mu$, transforming to a QuantumOperator list via the Jordan–Wigner transformation, and constructing the circuit for the exponential of each sub-term [Eq. (8)]. We note that optimization in QFORTE relies on the SciPy scientific computing library,⁶³ and that any string specifying a valid SciPy optimizer may be passed to the run() function of a VQE algorithm. The ordering of the operators $e^{t_\mu \hat{\kappa}_\mu}$ entering Eq. (18) is defined by the binary representation of the corresponding determinants $|\Phi_\mu\rangle = \hat{\tau}_\mu |\Phi_{\text{HF}}\rangle$ in the occupation number representation. The maximum excitation level (single and double, triple, etc. . .) for the operators in Eq. (18) can be of arbitrary rank and is specified by the user as an option passed to the run() function.

3.2 Adaptive VQE. We have also implemented the ADAPT-VQE approach, and adaptive variant of dUCC-VQE.³⁵ In ADAPT-VQE, the unitary ansatz at macro-iteration k is defined as

$$\hat{U}_{\text{ADAPT}}^{(k)}(\mathbf{t}) = \prod_\nu e^{t_\nu^{(k)} \hat{\kappa}_\nu^{(k)}} \quad (19)$$

where ν is a compound index corresponding to operators $\hat{\kappa}_\nu$ in a pool \mathcal{P} . In QFORTE it is possible to construct \mathcal{P} in a variety of ways, including the generalized single and double excitation/de-excitation operators described in the original publication.³⁵ The parameters $t_\nu^{(k)}$ are optimized at each macro-iteration employing the general VQE schema. New operators are determined from the pool by computing the energy gradient

$$g_\nu = \langle \Psi_{\text{VQE}} | [\hat{\mathcal{H}}, \hat{\kappa}_\nu] | \Psi_{\text{VQE}} \rangle \quad (20)$$

with respect to t_ν of each operator in \mathcal{P} and selecting the operator with the largest gradient magnitude. This new operator is placed at the end of the ansatz in the next iteration, and the procedure is terminated when the norm of the gradient vector for the pool falls below a user-provided threshold that controls the accuracy of the ansatz.

3.3 Projective quantum eigensolver (PQE) based on dUCC trial states. In the dUCC projective quantum eigensolver approach we consider a trial state of the form $|\Psi\rangle = \hat{U}(\mathbf{t}) |\Phi_0\rangle$, where $\hat{U}(\mathbf{t})$ is defined by Eq. (18). PQE aims to solve the following unitarily-transformed version of the Schrödinger equation, obtained from the original one by left-multiplying with $\hat{U}^\dagger(\mathbf{t})$,

$$\hat{U}^\dagger(\mathbf{t}) \hat{\mathcal{H}} \hat{U}(\mathbf{t}) |\Phi_0\rangle = E |\Phi_0\rangle \quad (21)$$

Rather than accomplishing this via variational minimization (as is done in VQE), PQE seeks to minimize the residual condition

$$r_\mu(\mathbf{t}) \equiv \langle \Phi_\mu | \hat{U}^\dagger(\mathbf{t}) \hat{\mathcal{H}} \hat{U}(\mathbf{t}) | \Phi_0 \rangle = 0, \text{ for all } \Phi_\mu \in Q \quad (22)$$

where the residual $r_\mu(\mathbf{t})$ is given by the projection of the unitarily-transformed Schrödinger equation onto the excited determinant $|\Phi_\mu\rangle$. In practice we only consider enforcing the residual condition for a subset Q of excited determinants (such as all single and double excitations).

The residuals r_μ can be easily determined from symmetric

expectation values and can therefore be measured via operator averaging on a quantum device. Specifically, each element r_μ is obtained as

$$\begin{aligned} r_\mu(\mathbf{t}) &= \langle \Omega_\mu | \hat{U}^\dagger(\mathbf{t}) \hat{H} \hat{U}(\mathbf{t}) | \Omega_\mu \rangle \\ &\quad - \frac{1}{2} \langle \Phi_0 | \hat{U}^\dagger(\mathbf{t}) \hat{H} \hat{U}(\mathbf{t}) | \Phi_0 \rangle \\ &\quad - \frac{1}{2} \langle \Phi_\mu | \hat{U}^\dagger(\mathbf{t}) \hat{H} \hat{U}(\mathbf{t}) | \Phi_\mu \rangle \end{aligned} \quad (23)$$

where Ω_μ is an easily preparable superposition of $|\Phi_0\rangle$ and $|\Phi_\mu\rangle$

$$|\Omega_\mu\rangle = e^{\frac{\pi}{4} \hat{k}_\mu} |\Phi_0\rangle = \frac{1}{\sqrt{2}} |\Phi_0\rangle + \frac{1}{\sqrt{2}} |\Phi_\mu\rangle \quad (24)$$

One of the most important features of dUCC-PQE is that the parameter vector \mathbf{t} can be updated by measuring the residuals via a simple quasi-Newton iteration approach

$$t_\mu^{(n+1)} = t_\mu^{(n)} + \frac{r_\mu^{(n)}}{\Delta_\mu} \quad (25)$$

where the superscript “(n)” indicates the amplitude at iteration n . The quantities Δ_μ are standard Møller–Plesset denominators $\Delta_\mu \equiv \Delta_{ij\dots}^{ab\dots} = \epsilon_i + \epsilon_j + \dots - \epsilon_a - \epsilon_b \dots$ where ϵ_i are Hartree–Fock orbital energies.

3.4 Selected PQE. The selected ansatz variation of PQE (SPQE) is also implemented in QFORTE and, similarly to ADAPT, it utilizes a dUCC ansatz constructed iteratively from a (growing) set of operators \mathcal{A} . In brief, the selection procedure is done by construction of a normalized state $|\tilde{r}\rangle$ defined as

$$\begin{aligned} |\tilde{r}\rangle &= \hat{U}^\dagger(\mathbf{t}) e^{i\Delta t \hat{H}} \hat{U}(\mathbf{t}) |\Phi_0\rangle \\ &= (1 + i\Delta t \hat{U}^\dagger(\mathbf{t}) \hat{H} \hat{U}(\mathbf{t})) |\Phi_0\rangle + \mathcal{O}(\Delta t^2) \end{aligned} \quad (26)$$

for which the square moduli of its probability amplitudes $|C_\mu|^2 \approx (\Delta t)^2 |\langle \Phi_\mu | \hat{U}^\dagger(\mathbf{t}) \hat{H} \hat{U}(\mathbf{t}) | \Phi_0 \rangle|^2$ are proportional to residuals r_μ . In QFORTE the time step is taken as a parameter of the calculation and the Suzuki–Trotter approximation^{64,65} is used for the time evolution operator. We may then approximate the values of the (normalized) squared residuals as

$$|\tilde{r}_\mu|^2 \approx \frac{N_\mu}{M} \quad (27)$$

where N_μ is the number of times the state $|\Phi_\mu\rangle$ is measured from M preparations of $|\tilde{r}\rangle$. A cumulative thresholding procedure is then utilized to add new operators \hat{k}_μ (corresponding to $|\tilde{r}_\mu|^2$) to the ansatz, enforcing the condition

$$\sum_{\hat{k}_\mu \notin \mathcal{A}}^{\text{excluded}} |r_\mu|^2 \approx \sum_{\hat{k}_\mu \notin \mathcal{A}}^{\text{excluded}} \frac{|\tilde{r}_\mu|^2}{\Delta t^2} \leq \Omega^2 \quad (28)$$

where Ω is a user-specified convergence threshold parameter. This selection strategy is particularly appealing for strongly correlated systems because it does not require the candidate operators \hat{k}_μ to be restricted to any particular excitation order.

3.5 Quantum imaginary time evolution. The quantum imaginary time evolution (QITE) algorithm¹³ obtains the ground state $|\Psi_0\rangle$ by propagating a trial state $|\Phi\rangle$ (assuming $\langle \Psi_0 | \Phi \rangle \neq 0$) via imaginary time evolution $e^{-\beta \hat{H}}$ in the limit of infinite propagation time,

$$|\Psi_0\rangle = \lim_{\beta \rightarrow \infty} \frac{1}{\sqrt{N(\beta)}} e^{-\beta \hat{H}} |\Phi\rangle \quad (29)$$

The factor $1/\sqrt{N(\beta)} = |\langle \Phi | e^{-2\beta \hat{H}} | \Phi \rangle|^{-1/2}$ guarantees normalization of the evolved state. Since the imaginary time evolution operator is non-unitary, its direct implementation on quantum computers is impractical. QITE circumvents this limitation by constructing a unitary that approximates the action of the imaginary time evolution operator for a small time step $\Delta\beta$. This unitary is obtained by matching a state propagated from imaginary time β to $\beta + \Delta\beta$ with the unitary $\exp(-i\Delta\beta \hat{A})$, where \hat{A} is Hermitian:

$$|\psi(\beta + \Delta\beta)\rangle = N(\Delta\beta)^{-1/2} e^{-\Delta\beta \hat{H}} |\psi(\beta)\rangle = e^{-i\Delta\beta \hat{A}} |\psi(\beta)\rangle \quad (30)$$

The operator \hat{A} can be written as a linear expansion of Pauli strings $\hat{\rho}_\mu = \prod_l \hat{\sigma}_{\mu_l}^{(l)}$ such that $\hat{A} = \sum_{\mu \in \mathcal{P}} \alpha_\mu \hat{\rho}_\mu$. Here, \mathcal{P} is a subset with dimension M of all possible $4^{N_{\text{qb}}}$ Pauli strings, $\mu \equiv (\mu_1, \mu_2, \dots, \mu_{N_{\text{qb}}})$ is a multi-index describing a unique Pauli operator product, and $\mu_l \in \{I, X, Y, Z\}$. Equations for QITE are obtained by expanding Eq. (30) up to linear terms and left-projecting onto $\langle \Phi | \hat{A}^\dagger$, yielding the M -dimensional linear system $\mathbf{S}\boldsymbol{\alpha} = \mathbf{b}$. The elements of \mathbf{S} , and \mathbf{b} , as well as the value of $N(\Delta\beta)$ can be determined via measurement of simple symmetric expectation values:¹³

$$N(\Delta\beta) \approx 1 - 2\Delta\beta \langle \Phi | \hat{H} | \Phi \rangle \quad (31)$$

$$S_{\mu\nu} = \langle \Phi | \hat{\rho}_\mu^\dagger \hat{\rho}_\nu | \Phi \rangle \quad (32)$$

and,

$$b_\mu = \frac{-i}{\sqrt{N(\Delta\beta)}} \langle \Phi | \hat{\rho}_\mu^\dagger \hat{H} | \Phi \rangle \quad (33)$$

Here $|\Phi\rangle$ is an approximation to the exact time evolved state $|\psi(\beta)\rangle$. We note that the overall QITE procedure is iterative, and requires that the linear system be solved $M = \beta/\Delta\beta$ times to reach the target evolution time β .

In QFORTE, the Pauli strings that enter into \mathcal{P} are generated automatically from a user-specified manifold of second-quantized operators. Specifically, given a set of excitation/de-excitation operators, these are first Jordan–Wigner transformed, and all unique terms containing an odd number of Y gates are included in \mathcal{P} . We note that the QFORTE implementation of QITE differs from the “inexact QITE” described in Ref. 13, in which a subgroup of important Pauli operators is chosen for each k -local Hamiltonian term.

3.6 Quantum Lanczos. The quantum Lanczos algorithm expands an eigenstate as a linear combination of states obtained via QITE:

$$|\Psi\rangle = \sum_{n=0}^M c_n |\psi(\beta_n)\rangle \quad (34)$$

Variational minimization leads to the generalized eigenvalue problem $\mathbf{Hc} = \mathbf{Sc}E$, where the matrix elements $(\mathbf{H})_{mn} = \langle \psi(\beta_m) | \hat{\mathcal{H}} | \psi(\beta_n) \rangle$ and $(\mathbf{S})_{mn} = \langle \psi(\beta_m) | \psi(\beta_n) \rangle$, with $\beta_m = m\Delta\beta$, are obtained from the QITE subroutine. A convenient feature of QL is that the matrix elements can be (approximately) evaluated in terms of the normalization coefficients N and symmetric energy expectation values:

$$S_{mn} \approx \langle \Phi | e^{-m\Delta\beta\hat{A}} e^{-n\Delta\beta\hat{A}} | \Phi \rangle = \frac{N(\beta_m)N(\beta_n)}{N^2(\beta_k)} \quad (35)$$

and,

$$\begin{aligned} H_{mn} &\approx \langle \Phi | e^{-m\Delta\beta\hat{A}} \hat{\mathcal{H}} e^{-n\Delta\beta\hat{A}} | \Phi \rangle \\ &= \frac{N(\beta_m)N(\beta_n)}{N^2(\beta_k)} \langle \psi(\beta_k) | \hat{\mathcal{H}} | \psi(\beta_k) \rangle \end{aligned} \quad (36)$$

where $2k = m + n$. This is a significant simplification that allows the determination of all quantities needed for QLanczos *without* using ancilla qubits.

3.7 Quantum Krylov (QK). In quantum Krylov diagonalization, a general state is written as a linear combination of the basis $\{\psi_n\}$ generated from real-time Hamiltonian evolutions at a given set of $s + 1$ time steps $\{t_1, t_2, \dots, t_s\}$ (typically chosen of the form $t_n = n\Delta t$) as

$$|\Psi\rangle = \sum_{n=0}^s c_n |\psi_n\rangle = \sum_{n=0}^s c_n e^{-it_n \hat{\mathcal{H}}} |\Phi\rangle \quad (37)$$

Variational minimization of the energy of the state Ψ leads to a generalized eigenvalue problem (like in the case of QLanczos) $\mathbf{Hc} = \mathbf{Sc}E$, where the elements of the overlap matrix (\mathbf{S}) and Hamiltonian (\mathbf{H}) are given by $S_{mn} = \langle \psi_m | \psi_n \rangle$ and $H_{mn} = \langle \psi_m | \hat{\mathcal{H}} | \psi_n \rangle$, respectively. In QFORTE the quantum circuit used to approximate the time evolution is generated via Eq. (8) using the Suzuki-Trotter decomposition

$$e^{-it\hat{\mathcal{H}}} = e^{-it \sum_\ell \theta_\ell \hat{P}_\ell} \approx \left(\prod_\ell e^{-i\theta_\ell \hat{P}_\ell / r} \right)^r \quad (38)$$

with r Trotter steps. The quantum circuits used to evaluate \mathbf{S} and \mathbf{H} are implemented in QFORTE via a variant of the Hadamard test, requiring only an additional ancillary qubit.⁶⁶ In QFORTE the time step (Δt), number of time evolutions states (s), and number of Trotter steps (r) are all given as user-specified values. We note that it is also possible to perform the exact time evolution operation (as opposed to those resulting from Trotterized dynamics) in QFORTE using sparse matrix operations.

3.8 Multireference selected QK. A selected multireference variant of QK (MRSQK) is also implemented in QFORTE. The base procedure is identical to that of QK described in the above section, but several orthogonal reference states $|\Phi_I\rangle$ are included in the subspace and time evolved in order to improve numerical stability and target states with multireference character. The MRSQK wave function is thus given

by

$$|\Psi\rangle = \sum_\alpha c_\alpha |\psi_\alpha\rangle = \sum_{I=1}^d \sum_{n=0}^s c_I^{(n)} e^{-it_n \hat{\mathcal{H}}} |\Phi_I\rangle \quad (39)$$

In MRSQK, a preliminary single-reference QK calculation is performed in order to determine the set of important references. The resulting single-reference QK wave function $|\tilde{\Psi}\rangle = \sum_n \tilde{c}_n |\psi_n\rangle$ is used to construct a list of determinants with importance value $P_\mu = |\langle \phi_\mu | \tilde{\Psi} \rangle|^2$, since the probability of measuring a determinant ϕ_μ is equal to $P_\mu = |\langle \phi_\mu | \tilde{\Psi} \rangle|^2$. In QFORTE, the quantity P_μ is approximated by measuring each element of the Krylov basis and estimating the total probability as a weighted sum over references via

$$P_\mu = \left| \sum_\alpha \langle \phi_\mu | \psi_\alpha \rangle c_\alpha \right|^2 \approx \sum_\alpha |\langle \phi_\mu | \psi_\alpha \rangle|^2 |c_\alpha|^2 \quad (40)$$

Once formed, the list of the most important determinants is augmented to guarantee that all spin arrangements of open-shell determinants are included, and the d most important references are used in the MRSQK subspace. The number of references (d), the MRSQK time step Δt_{mr} , the number of time evolutions per reference (s), and the parameters for the preliminary single-reference QK calculation are all specified by the user at runtime.

4. REPRESENTATIVE TIMINGS

By implementing an optimized low-level state-vector simulator, the algorithms implemented in QFORTE can be applied in a reasonable amount of time on small-sized molecular systems. This enables the rapid development and generation of paper-quality benchmark data for new algorithms implemented in QFORTE. To illustrate this point, we report timings for operations common to many quantum algorithms, such as application of circuits and evaluation of expectation values. As an example, we consider the cost to generate a state-vector corresponding to a disentangled UCC ansatz (see Eq. 18) with particle-hole single and double excitations (dUCCSD) for a family of molecular hydrogen systems $\text{H}_2\text{--H}_{10}$. The dUCCSD state is produced by applying the corresponding unitary \hat{U}_{SD} to a Hartree-Fock reference. In this example, we employ a minimum basis set, corresponding to computations on 4–20 qubits. We also consider the time required to evaluate the Hamiltonian expectation value of the dUCCSD state via exact operator averaging: $\langle \mathcal{H}_q \rangle = \sum_\ell^{N_{\text{ps}}} h_\ell \langle \hat{P}_\ell \rangle$. Figure 5 shows that QFORTE can accomplish such operations on the order of fractions of a second to a few minutes (on a laptop computer) for the systems considered here. In particular, operations on systems with 6 electrons can be performed in the order of less than a second, enabling rapid testing of algorithms on relatively complex problems.

5. EXAMPLE: DEVELOPING NEW ALGORITHMS WITH QFORTE

In this section we discuss some examples of how QFORTE can be used to facilitate the implementation of new quantum algorithms. We also then show how QFORTE can be used to produce comparative studies of different algorithms. In addition to the example described below, QFORTE has several

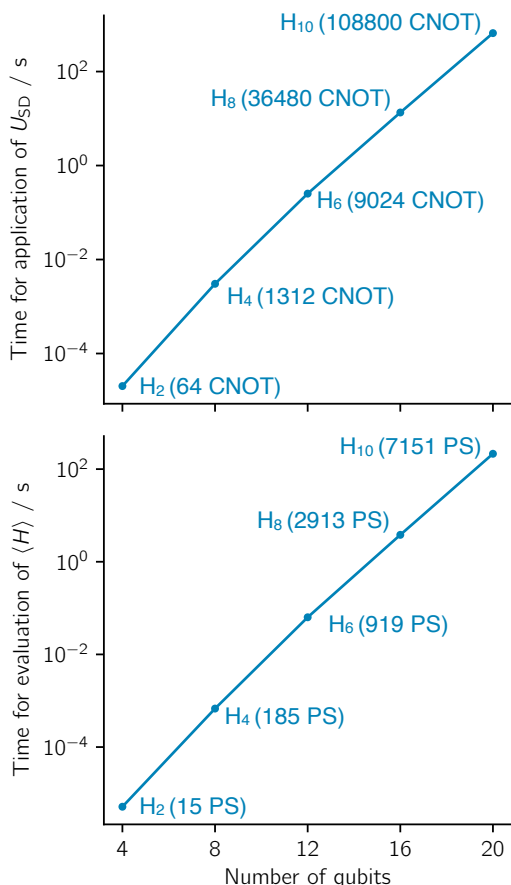


Figure 5: Timings for (top) the application of disentangled UCCSD circuits to a quantum states of increasing dimension, and for (bottom) the evaluation of the molecular hydrogen Hamiltonians of increasing size (H₂–H₁₀). The number of CNOT gates in the dUCCSD circuits and the number of Pauli strings (PS) in the Hamiltonian are reported in parentheses beside the corresponding systems in the top and bottom plots, respectively. All cluster amplitudes in the dUCCSD circuits were initialized to 1.0. All timings shown were generated on a laptop computer with an Intel i5 3.1 GHz processor.

Jupyter-notebook tutorials available on topics ranging from basic API use, to detailed instructions for various algorithm implementations, to running jobs in a black-box fashion.

As an example, we consider the workflow necessary to experiment with a new VQE ansatz based on the theory of paired CC doubles.^{67,68} We will formulate the ansatz in the disentangled unitary coupled cluster form [Eq. (18)], such that operators entering into the resulting (disentangled) paired UCC doubles (p-dUCCD) ansatz maintain a seniority-zero trial state (include only contributions from closed-shell determinants). We would also like to enforce that the ansatz include only particle-hole excitations/de-excitations, such that the final ansatz has the form:

$$\hat{U}_{\text{p-dUCCD}}(\mathbf{t}) = \prod_i^{\text{occ}} \prod_a^{\text{vir}} e^{t_i^a (\hat{a}_{i\beta}^\dagger \hat{a}_{i\alpha}^\dagger \hat{a}_{a\alpha} \hat{a}_{a\beta} - \hat{a}_{a\beta}^\dagger \hat{a}_{a\alpha}^\dagger \hat{a}_{i\alpha} \hat{a}_{i\beta})} \quad (41)$$

where the indices i , and a pertain to occupied or virtual spatial orbitals, respectively, for a specified Hartree-Fock reference

state.

The Python class structure in QFORTE can easily facilitate the implementation of the p-dUCCD-VQE variant. To begin, we define a mixin class (pdUCCD) that defines only the function `ansatz_circuit()`, responsible for returning the parameterized unitary circuit $\hat{U}_{\text{p-dUCCD}}(\mathbf{t})$ comprised of gates of the form shown in Fig. 4 for the exponentials of Pauli-strings. The `ansatz_circuit()` function provided by the mixin class will be called by the function `AnsatzAlgorithm.energy_feval()` which applies $\hat{U}_{\text{p-dUCCD}}(\mathbf{t})$ to a `Computer()` (initialized to the Hartree-Fock reference) and returns the energy expectation value (without noise by default). Next, we define a new class `pdUCCDVQE` derived from the VQE abstract base class and the `pdUCCD` mixin class. Once the `pdUCCDVQE` child class is defined, we simply need to define two functions: `run()` and `solve()`. The `run()` function takes the user-defined parameters such as convergence thresholds, argument D (number of layers), defines algorithm specific attributes such as the number of occupied and virtual orbitals, and calls all necessary subroutines to run the algorithm.

Finally, the `solve()` function calls the user-specified classical optimization algorithm (BFGS^{69–72} by default), and defines: (i) the number of classical parameters used, (ii) the number of CNOT gates in the ansatz circuit (without considering advanced compilation techniques⁷³), and (iii) to total number of Pauli-string evaluations ($\langle \Phi_0 | \hat{U}_{\text{p-dUCCD}}^\dagger(\mathbf{t}) \hat{P}_\ell \hat{U}_{\text{p-dUCCD}}(\mathbf{t}) | \Phi_0 \rangle$). An overview of the steps described above is given in Lst. 8. We note that in practice QFORTE requires that derived classes define network printing and attribute verification functions in addition to the three described above, but we do not show these in Lst. 8 for brevity.

After implementing the p-dUCCD-VQE method, we would like to compare it to other quantum algorithms, like VQE based on a conventional disentangled UCC ansatz. Once an algorithm has been implemented, running jobs in QFORTE is very simple, as we only need to pass a molecule object to an algorithm constructor (see Sec. 2.3). For example, Lst. 9 shows how to calculate the potential energy curve for H₄ using the new p-dUCCD-VQE method, VQE with a disentangled UCC single and double excitations ansatz (dUCCSD-VQE), dUCCSD optimized via PQE (dUCCSD-PQE), and quantum Krylov diagonalization with a Hartree-Fock reference (QK). After running the algorithms, it is possible to extract salient information such as the predicted energy, and computational resource estimates. Using the code in Lst. 9, we can produce the potential energy curve scans shown in Fig. 6 and obtain the computational resources estimates reported in Tab. 1. In this example, we conclude that although the p-dUCCD-VQE circuit is very compact (from a circuit depth and classical parameterization standpoint), it does not afford the same variational flexibility as the other dUCC-based methods or QK.

6. CONCLUSION

In this article we introduce the new open-source software package QFORTE. QFORTE aids the development and testing of quantum algorithms for molecular electronic structure,

```

1 from qforte import *
2 from scipy.optimize import minimize
3
4 class pdUCCD:
5     def ansatz_circuit(self, params):
6         Kq = QubitOperator()
7
8         for i in range(self._nocc):
9             for a in range(self._nvir):
10                mu = i*self._nocc + a
11                k_mu = SQOperator()
12                ia = 2*i
13                ib = 2*i+1
14                aa = 2*self._nocc + 2*a
15                ab = 2*self._nocc + 2*a+1
16                k_mu.add( 1.0*params[mu], [ab, aa], [ia, ib])
17                k_mu.add(-1.0*params[mu], [ib, ia], [aa, ab])
18                Kq.add(k_mu.jw_transform())
19
20        U, phase = trotterize(Kq)
21        return U
22
23 class pdUCCDVQE(pdUCCD, VQE):
24     def run(self, optimizer='BFGS'):
25         self._optimizer = optimizer
26         self._nocc = int(sum(self._ref) / 2)
27         self._nvir = int((self._nqb - sum(self._ref)) / 2)
28         self._npar = int(self._nocc*self._nvir)
29         self._params_0 = [0.0 for k in range(self._npar)]
30         self.solve()
31
32     def solve(self):
33         res = minimize(self.energy_feval, self._params_0, method=self._optimizer)
34         self._final_res = res
35         self._Egs = res.fun
36         self._n_classical_params = len(res.x)
37         self._n_cnot = self.build_Uvqc(res.x).get_num_cnots()
38         self._Umaxdepth = self.build_Uvqc(res.x)
39         self._n_pauli_trm_measures = self._Nl * res.nfev

```

Listing 8: Example Python code i) defining a mixin class pdUCCD responsible for the construction of the circuit for the p-dUCCD ansatz, and ii) defining a derived pdUCCDVQE class responsible for the optimization of the ansatz. Note that QFORTE requires that all derived classes additionally define printing and attribute verification functions in addition to those shown here.

```

1 from qforte import *
2 import numpy as np
3
4 for r in np.linspace(0.5, 2.0, 30):
5
6     # Specify geometry as a function of r.
7     geom = [('H', (0., 0., 0.0)),
8             ('H', (0., 0., 1*r)),
9             ('H', (0., 0., 2*r)),
10            ('H', (0., 0., 3*r))]
11
12    # Run classical scf with Psi4 backend.
13    mol = system_factory(build_type='psi4', mol_geometry=geom, basis='sto-3g')
14
15    # Instantiate and run new VQE algorithm.
16    pdUCCD_VQE = pdUCCDVQE(mol)
17    pdUCCD_VQE.run()
18
19    # Instantiate and run black-box algorithms.
20    dUCCSD_VQE = UCCNVQE(mol)
21    dUCCSD_VQE.run(pool_type='SD', opt_thresh = 1.0e-4)
22
23    dUCCSD_PQE = UCCNVQE(mol)
24    dUCCSD_PQE.run(pool_type='SD', res_vec_thresh = 1.0e-4)
25
26    QK = SRQK(mol)
27    QK.run(s=3)

```

Listing 9: Example of how to compute a potential energy curve of the linear H_4 molecule using both the pdUCCDVQE algorithm implemented in List. 8 and various black-box algorithms implemented in QFORTE.

Table 1: Computational resource estimates and mean signed error for p-dUCCD-VQE, dUCCSD-VQE, dUCCSD-PQE and QK($s=3$, $\Delta t = 0.5$ a.u.) computed for the dissociation of linear H_4 in a STO-3G basis. N_{par} is the number of classical parameters used in the ansatz circuit for VQE/PQE or the dimension of the generalized eigenvalue problem for QK, N_{CNOT} is the number of CNOT gates in the ansatz (for VQE/PQE) or Trotterized time-evolution circuit (for QK), \bar{N}_{PSE} is the average number of Pauli-string evaluations over the entire potential energy curve, and MSE is the mean signed energy error (in mE_h , with respect to the exact energy) computed over the entire potential curve (H-H near-neighbor bond distances in the range 0.5–2.0 Å).

| Method | N_{par} | N_{CNOT} | \bar{N}_{PSE} | MSE (mE_h) |
|-------------|------------------|-------------------|------------------------|----------------|
| p-dUCCD-VQE | 4 | 192 | 11063 | 80.922 |
| dUCCSD-VQE | 14 | 736 | 134804 | 1.204 |
| dUCCSD-PQE | 14 | 736 | 94283 | 1.204 |
| QK | 4 | 2656 | 2972 | 23.483 |

and has been used by our research group to implement the algorithms introduced in Refs. 42 and 44. The ability of QFORTE to facilitate black-box calculations with a wide variety of quantum algorithms using only a classical electronic structure package as a dependency makes it an ideal tool for comparing quantum algorithms based on the accuracy of their outputs and their required computational resources. Moreover, the easy-to-use basic components (implemented as C++ classes exposed in Python) combined with a simple Python class structure allow QFORTE to function as an excellent platform for implementing and testing new quantum

algorithms.

In the future, we plan to expand the features and quantum algorithms implemented in QFORTE with the hope that its unique capabilities will provide a useful tool to other researchers. For example, we plan to add support in the low-level layer of QFORTE for spin and point-group symmetries and enable the treatment of open-shell systems. Another desirable feature is supporting fermionic encodings beyond the currently-available Jordan-Wigner transformation. On the front of the simulator performance, a significant speedup could be achieved by applying particle number and spin symmetry restrictions to the state vector, such that the application of fermionic operators can be performed efficiently using well-established quantum chemistry techniques,⁷⁴ extending the scope of routine computation to systems with more than 24 qubits. Such an approach has recently been realized as a python implementation in the so-called fermionic quantum emulator,²¹ but has yet to be implemented in a compiled language.

On the algorithm side, we plan to extend the type of ansätze supported in QFORTE (see, e.g., Refs. 33,34,75–77). We are also interested in implementing additional excited-state methods (see, e.g., Refs. 37,54,78,79). In addition to new algorithms and ansätze, we also aim in the future to implement techniques for quantum resource reduction such as qubit tapering,⁸⁰ Hamiltonian factorization,⁸¹ and circuit compilation.⁷³ It is our hope that QFORTE will become a valuable asset to the quantum simulation community. We welcome feedback and contributions from any who wish to

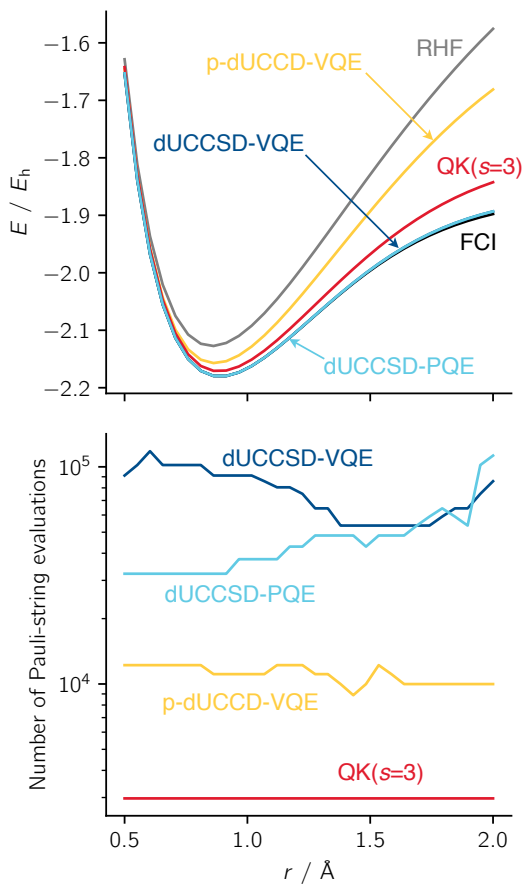


Figure 6: Ground state potential energy curve (top) and number of Pauli-string evaluations (bottom) computed with the p-dUCCD-VQE method implemented in Lst. 8, dUCCSD-VQE, dUCCSD-PQE, and QK with three time evolved basis states for the dissociation of linear H_4 in a STO-3G basis. The QK calculation used a time step of $\Delta t = 0.5$ a.u. and a Trotterized time evolution circuit with a single Trotter step ($r = 1$). The restricted Hartree-Fock (RHF) and FCI curves are also reported for reference.

see their work represented in our package.

Acknowledgement This work was supported by the U.S. Department of Energy under Award No. DE-SC0019374. N.H.S. was supported by a fellowship from The Molecular Sciences Software Institute under NSF grant ACI-1547580. QFORTE was predominantly developed as a Molecular Sciences Software Institute fellowship project. N.H.S. would like to thank his mentor at the institute Jonathan Moussa for his thoughts and advice. In addition to development by N.H.S. and F.A.E., the authors acknowledge contributions to the QFORTE code from Nan He, Renke Huang, Jonathon Misiewicz, and Ilias Magoulas.

REFERENCES

- (1) Arute, F.; Arya, K.; Babbush, R.; Bacon, D.; Bardin, J. C.; Barends, R.; Biswas, R.; Boixo, S.; Brandao, F. G.; Buell, D. A. Quantum supremacy using a programmable superconducting processor. *Nature* **2019**, *574*, 505–510.
- (2) O’Malley, P. J. J.; Babbush, R.; Kivlichan, I. D.; Romero, J.; McClean, J. R.; Barends, R.; Kelly, J.; Roushan, P.; Tranter, A.; Ding, N.; Campbell, B.; Chen, Y.; Chen, Z.; Chiaro, B.; Dunsworth, A.; Fowler, A. G.; Jeffrey, E.; Lucero, E.; Megrant, A.; Mutus, J. Y.; Neeley, M.; Neill, C.; Quintana, C.; Sank, D.; Vainsencher, A.; Wenner, J.; White, T. C.; Coveney, P. V.; Love, P. J.; Neven, H.; Aspuru-Guzik, A.; Martinis, J. M. Scalable Quantum Simulation of Molecular Energies. *Phys. Rev. X* **2016**, *6*, 031007.
- (3) Kandala, A.; Mezzacapo, A.; Temme, K.; Takita, M.; Brink, M.; Chow, J. M.; Gambetta, J. M. Hardware-efficient variational quantum eigensolver for small molecules and quantum magnets. *Nature* **2017**, *549*, 242–246.
- (4) Colless, J. I.; Ramasesh, V. V.; Dahlen, D.; Blok, M. S.; Kimchi-Schwartz, M.; McClean, J.; Carter, J.; De Jong, W.; Siddiqi, I. Computation of molecular spectra on a quantum processor with an error-resilient algorithm. *Phys. Rev. X* **2018**, *8*, 011021.
- (5) Shen, Y.; Zhang, X.; Zhang, S.; Zhang, J.-N.; Yung, M.-H.; Kim, K. Quantum implementation of the unitary coupled cluster for simulating molecular electronic structure. *Phys. Rev. A* **2017**, *95*, 020501.
- (6) Hempel, C.; Maier, C.; Romero, J.; McClean, J.; Monz, T.; Shen, H.; Jurcevic, P.; Lanyon, B. P.; Love, P.; Babbush, R., et al. Quantum chemistry calculations on a trapped-ion quantum simulator. *Phys. Rev. X* **2018**, *8*, 031022.
- (7) Nam, Y.; Chen, J.-S.; Pienti, N. C.; Wright, K.; Delaney, C.; Maslov, D.; Brown, K. R.; Allen, S.; Amini, J. M.; Apisdorf, J., et al. Ground-state energy estimation of the water molecule on a trapped-ion quantum computer. *npj Quantum Inf.* **2020**, *6*, 1–6.
- (8) Lin, C. Y.-Y.; Zhu, Y. Performance of QAOA on typical instances of constraint satisfaction problems with bounded degree. *arXiv preprint arXiv:1601.01744* **2016**,
- (9) Wang, Z.; Hadfield, S.; Jiang, Z.; Rieffel, E. G. Quantum approximate optimization algorithm for maxcut: A fermionic view. *Phys. Rev. A* **2018**, *97*, 022304.
- (10) Preskill, J. Quantum Computing in the NISQ era and beyond. *Quantum* **2018**, *2*, 79.

- (11) Peruzzo, A.; McClean, J.; Shadbolt, P.; Yung, M.-H.; Zhou, X.-Q.; Love, P. J.; Aspuru-Guzik, A.; O'Brien, J. L. A variational eigenvalue solver on a photonic quantum processor. *Nat. Commun.* **2014**, *5*, 4213.
- (12) McClean, J. R.; Romero, J.; Babbush, R.; Aspuru-Guzik, A. The theory of variational hybrid quantum-classical algorithms. *New J. Phys.* **2016**, *18*, 023023.
- (13) Motta, M.; Sun, C.; Tan, A. T.; O'Rourke, M. J.; Ye, E.; Minnich, A. J.; Brandão, F. G.; Chan, G. K.-L. Determining eigenstates and thermal states on a quantum computer using quantum imaginary time evolution. *Nat. Phys.* **2019**, *16*, 1–6.
- (14) McArdle, S.; Endo, S.; Aspuru-Guzik, A.; Benjamin, S. C.; Yuan, X. Quantum computational chemistry. *Rev. Mod. Phys.* **2020**, *92*, 015003.
- (15) Bauer, B.; Bravyi, S.; Motta, M.; Kin-Lic Chan, G. Quantum algorithms for quantum chemistry and quantum materials science. *Chem. Rev.* **2020**, *120*, 12685–12717.
- (16) Aleksandrowicz, G.; Alexander, T.; Barkoutsos, P.; Bello, L.; Ben-Haim, Y.; Bucher, D.; Cabrera-Hernández, F. J.; Carballo-Franquis, J.; Chen, A.; Chen, C.-F.; Chow, J. M.; Córcoles-Gonzales, A. D.; Cross, A. J.; Cross, A.; Cruz-Benito, J.; Culver, C.; González, S. D. L. P.; Torre, E. D. L.; Ding, D.; Dumitrescu, E.; Duran, I.; Eendebak, P.; Everitt, M.; Sertage, I. F.; Frisch, A.; Fuhrer, A.; Gambetta, J.; Gago, B. G.; Gomez-Mosquera, J.; Greenberg, D.; Hamamura, I.; Havlicek, V.; Hellmers, J.; Łukasz Herok; Horii, H.; Hu, S.; Imamichi, T.; Itoko, T.; Javadi-Abhari, A.; Kanazawa, N.; Karazeev, A.; Krulich, K.; Liu, P.; Luh, Y.; Maeng, Y.; Marques, M.; Martín-Fernández, F. J.; McClure, D. T.; McKay, D.; Meesala, S.; Mezzacapo, A.; Moll, N.; Rodríguez, D. M.; Nannicini, G.; Nation, P.; Ollitrault, P.; O'Riordan, L. J.; Paik, H.; Pérez, J.; Phan, A.; Pistoia, M.; Prutyanov, V.; Reuter, M.; Rice, J.; Davila, A. R.; Rudy, R. H. P.; Ryu, M.; Sathaye, N.; Schnabel, C.; Schoute, E.; Setia, K.; Shi, Y.; Silva, A.; Siraichi, Y.; Sivarajah, S.; Smolin, J. A.; Soeken, M.; Takahashi, H.; Tavernelli, I.; Taylor, C.; Taylour, P.; Trabing, K.; Treinish, M.; Turner, W.; Vogt-Lee, D.; Vuillot, C.; Wildstrom, J. A.; Wilson, J.; Winston, E.; Wood, C.; Wood, S.; Wörner, S.; Akhalwaya, I. Y.; Zoufal, C. Qiskit: An Open-source Framework for Quantum Computing. **2019**,
- (17) Developers, C. Cirq. 2021; <https://doi.org/10.5281/zenodo.4750446>, See full list of authors on Github: <https://github.com/quantumlib/Cirq/graphs/contributors>.
- (18) Microsoft, The qsharp user guide - microsoft quantum. **2020**,
- (19) Smith, R. S.; Curtis, M. J.; Zeng, W. J. A practical quantum instruction set architecture. *arXiv preprint arXiv:1608.03355* **2016**,
- (20) Killoran, N.; Izaac, J.; Quesada, N.; Bergholm, V.; Amy, M.; Weedbrook, C. Strawberry fields: A software platform for photonic quantum computing. *Quantum* **2019**, *3*, 129.
- (21) Rubin, N. C.; Shiozaki, T.; Throssell, K.; Chan, G. K.; Babbush, R. The Fermionic Quantum Emulator. *arXiv preprint arXiv:2104.13944* **2021**,
- (22) McClean, J.; Rubin, N.; Sung, K.; Kivlichan, I. D.; Bonet-Monroig, X.; Cao, Y.; Dai, C.; Fried, E. S.; Gidney, C.; Gimby, B., et al. OpenFermion: the electronic structure package for quantum computers. *Quantum Sci. Technol.* **2020**,
- (23) Smelyanskiy, M.; Sawaya, N. P.; Aspuru-Guzik, A. qHiPSTER: The quantum high performance software testing environment. *arXiv preprint arXiv:1601.07195* **2016**,
- (24) Luo, X.-Z.; Liu, J.-G.; Zhang, P.; Wang, L. Yao. jl: Extensible, efficient framework for quantum algorithm design. *Quantum* **2020**, *4*, 341.
- (25) Suzuki, Y.; Kawase, Y.; Masumura, Y.; Hiraga, Y.; Nakadai, M.; Chen, J.; Nakanishi, K. M.; Mitarai, K.; Imai, R.; Tamiya, S., et al. Qulacs: a fast and versatile quantum circuit simulator for research purpose. *arXiv preprint arXiv:2011.13524* **2020**,
- (26) Kottmann, J. S.; Alperin-Lea, S.; Tamayo-Mendoza, T.; Cervera-Lierta, A.; Lavigne, C.; Yen, T.-C.; Verteletskyi, V.; Schleich, P.; Anand, A.; Degroote, M., et al. Tequila: A platform for rapid development of quantum algorithms. *Quantum Sci. Technol.* **2021**, *6*, 024009.
- (27) Bergholm, V.; Izaac, J.; Schuld, M.; Gogolin, C.; Alam, M. S.; Ahmed, S.; Arrazola, J. M.; Blank, C.; Delgado, A.; Jahangiri, S., et al. PennyLane: Automatic differentiation of hybrid quantum-classical computations. *arXiv preprint arXiv:1811.04968* **2018**,
- (28) Steiger, D. S.; Häner, T.; Troyer, M. ProjectQ: an open source software framework for quantum computing. *Quantum* **2018**, *2*, 49.
- (29) Sun, Q.; Berkelbach, T. C.; Blunt, N. S.; Booth, G. H.; Guo, S.; Li, Z.; Liu, J.; McClain, J. D.; Sayfutyarova, E. R.; Sharma, S., et al. PySCF: the Python-based simulations of chemistry framework. *Wiley Interdiscip. Rev. Comput. Mol. Sci.* **2018**, *8*, e1340.
- (30) Smith, D. G.; Burns, L. A.; Simmonett, A. C.; Parrish, R. M.; Schieber, M. C.; Galvelis, R.; Kraus, P.; Kruse, H.; Di Remigio, R.; Alenaizan, A., et al. Psi4 1.4: Open-source software for high-throughput quantum chemistry. *J. Chem. Phys.* **2020**, *152*, 184108.

- (31) Barkoutsos, P. K.; Gonthier, J. F.; Sokolov, I.; Moll, N.; Salis, G.; Fuhrer, A.; Ganzhorn, M.; Egger, D. J.; Troyer, M.; Mezzacapo, A., et al. Quantum algorithms for electronic structure calculations: Particle-hole Hamiltonian and optimized wave-function expansions. *Phys. Rev. A* **2018**, *98*, 022322.
- (32) Romero, J.; Babbush, R.; McClean, J. R.; Hempel, C.; Love, P. J.; Aspuru-Guzik, A. Strategies for quantum computing molecular energies using the unitary coupled cluster ansatz. *Quantum Sci. Technol.* **2019**, *4*, 014008.
- (33) Wecker, D.; Hastings, M. B.; Troyer, M. Progress towards practical quantum variational algorithms. *Phys. Rev. A* **2015**, *92*, 042303.
- (34) Ryabinkin, I. G.; Yen, T.-C.; Genin, S. N.; Izmaylov, A. F. Qubit Coupled Cluster Method: A Systematic Approach to Quantum Chemistry on a Quantum Computer. *J. Chem. Theory Comput.* **2018**, *14*, 6317–6326.
- (35) Grimsley, H. R.; Economou, S. E.; Barnes, E.; Mayhall, N. J. An adaptive variational algorithm for exact molecular simulations on a quantum computer. *Nat. Commun.* **2019**, *10*, 1–9.
- (36) Ryabinkin, I. G.; Lang, R. A.; Genin, S. N.; Izmaylov, A. F. Iterative Qubit Coupled Cluster approach with efficient screening of generators. *J. Chem. Theory Comput.* **2020**, *16*, 1055–1063.
- (37) McClean, J. R.; Kimchi-Schwartz, M. E.; Carter, J.; de Jong, W. A. Hybrid quantum-classical hierarchy for mitigation of decoherence and determination of excited states. *Phys. Rev. A* **2017**, *95*, 042308.
- (38) Kitaev, A. Y. Quantum measurements and the Abelian stabilizer problem. *e-print arXiv:9511026 [quant-ph]* **1995**,
- (39) Abrams, D. S.; Lloyd, S. Simulation of Many-Body Fermi Systems on a Universal Quantum Computer. *Phys. Rev. Lett.* **1997**, *79*, 2586–2589.
- (40) Abrams, D. S.; Lloyd, S. Quantum algorithm providing exponential speed increase for finding eigenvalues and eigenvectors. *Phys. Rev. Lett.* **1999**, *83*, 5162–5165.
- (41) Parrish, R. M.; McMahon, P. L. Quantum Filter Diagonalization: Quantum Eigendecomposition without Full Quantum Phase Estimation. *e-print arXiv:1909.08925 [quant-ph]* **2019**,
- (42) Stair, N. H.; Huang, R.; Evangelista, F. A. A Multireference Quantum Krylov Algorithm for Strongly Correlated Electrons. *J. Chem. Theory Comput.* **2020**, *16*, 2236–2245.
- (43) Klymko, K.; Mejuto-Zaera, C.; Cotton, S. J.; Wudarski, F.; Urbanek, M.; Hait, D.; Head-Gordon, M.; Whaley, K. B.; Moussa, J.; Wiebe, N., et al. Real time evolution for ultracompact Hamiltonian eigenstates on quantum hardware. *arXiv preprint arXiv:2103.08563* **2021**,
- (44) Stair, N. H.; Evangelista, F. A. *PRX Quantum* **2021**, *2*, 030301.
- (45) Jakob, W.; Rhineland, J.; Moldovan, D. pybind11–Seamless operability between C++ 11 and Python. *URL: <https://github.com/pybind/pybind11>* **2017**,
- (46) Yung, M.-H.; Casanova, J.; Mezzacapo, A.; McClean, J.; Lamata, L.; Aspuru-Guzik, A.; Solano, E. From transistor to trapped-ion computers for quantum chemistry. *Sci. Rep.* **2014**, *4*, 3589.
- (47) Crawford, T. D.; Schaefer, H. F. An introduction to coupled cluster theory for computational chemists. *Rev. Comput. Chem.* **2000**, *14*, 33–136.
- (48) Jordan, P.; Wigner, E. P. *The Collected Works of Eugene Paul Wigner*; Springer, 1993; pp 109–129.
- (49) Bravyi, S. B.; Kitaev, A. Y. Fermionic quantum computation. *Ann. Phys.* **2002**, *298*, 210–226.
- (50) Havlíček, V.; Troyer, M.; Whitfield, J. D. Operator locality in the quantum simulation of fermionic models. *Phys. Rev. A* **2017**, *95*, 032332.
- (51) Setia, K.; Whitfield, J. D. Bravyi-Kitaev Superfast simulation of electronic structure on a quantum computer. *J. Chem. Phys.* **2018**, *148*, 164104.
- (52) Setia, K.; Bravyi, S.; Mezzacapo, A.; Whitfield, J. D. Superfast encodings for fermionic quantum simulation. *Phys. Rev. Res.* **2019**, *1*, 033033.
- (53) Cerezo, M.; Arrasmith, A.; Babbush, R.; Benjamin, S. C.; Endo, S.; Fujii, K.; McClean, J. R.; Mitarai, K.; Yuan, X.; Cincio, L., et al. Variational quantum algorithms. *arXiv preprint arXiv:2012.09265* **2020**,
- (54) Huggins, W. J.; Lee, J.; Baek, U.; O’Gorman, B.; Whaley, K. B. A non-orthogonal variational quantum eigensolver. *New J. Phys.* **2020**,
- (55) Evangelista, F. A.; Chan, G. K.-L.; Scuseria, G. E. Exact parameterization of fermionic wave functions via unitary coupled cluster theory. *J. Chem. Phys.* **2019**, *151*, 244112.
- (56) Szalay, P. G.; Nooijen, M.; Bartlett, R. J. Alternative ansätze in single reference coupled-cluster theory. III. A critical analysis of different methods. *J. Chem. Phys.* **1995**, *103*, 281–298.

- (57) Taube, A. G.; Bartlett, R. J. New perspectives on unitary coupled-cluster theory. *International journal of quantum chemistry* **2006**, *106*, 3393–3401.
- (58) Cooper, B.; Knowles, P. J. Benchmark studies of variational, unitary and extended coupled cluster methods. *J. Chem. Phys.* **2010**, *133*, 234102.
- (59) Evangelista, F. A. Alternative single-reference coupled cluster approaches for multireference problems: The simpler, the better. *J. Chem. Phys.* **2011**, *134*, 224102.
- (60) Harsha, G.; Shiozaki, T.; Scuseria, G. E. On the difference between variational and unitary coupled cluster theories. *J. Chem. Phys.* **2018**, *148*, 044107.
- (61) Schuld, M.; Bergholm, V.; Gogolin, C.; Izaac, J.; Killo-ran, N. Evaluating analytic gradients on quantum hardware. *Phys. Rev. A* **2019**, *99*, 032331.
- (62) Kottmann, J. S.; Anand, A.; Aspuru-Guzik, A. A Feasible Approach for Automatically Differentiable Unitary Coupled-Cluster on Quantum Computers. *arXiv preprint arXiv:2011.05938* **2020**,
- (63) Virtanen, P.; Gommers, R.; Oliphant, T. E.; Haberland, M.; Reddy, T.; Cournapeau, D.; Burovski, E.; Peterson, P.; Weckesser, W.; Bright, J., et al. SciPy 1.0: fundamental algorithms for scientific computing in Python. *Nat. Methods* **2020**, *17*, 261–272.
- (64) Trotter, H. F. On the product of semi-groups of operators. *Proc. Am. Math. Soc.* **1959**, *10*, 545–551.
- (65) Suzuki, M. Improved Trotter-like formula. *Phys. Lett. A* **1993**, *180*, 232–234.
- (66) Aharonov, D.; Jones, V.; Landau, Z. A polynomial quantum algorithm for approximating the Jones polynomial. *Algorithmica* **2009**, *55*, 395–421.
- (67) Limacher, P. A.; Ayers, P. W.; Johnson, P. A.; De Baerdemacker, S.; Van Neck, D.; Bultinck, P. A new mean-field method suitable for strongly correlated electrons: Computationally facile antisymmetric products of nonorthogonal geminals. *J. Chem. Theory Comput.* **2013**, *9*, 1394–1401.
- (68) Bulik, I. W.; Henderson, T. M.; Scuseria, G. E. Can single-reference coupled cluster theory describe static correlation? *J. Chem. Theory Comput.* **2015**, *11*, 3171–3179.
- (69) Broyden, C. G. The convergence of a class of double-rank minimization algorithms 1. general considerations. *IMA J. Appl. Math.* **1970**, *6*, 76–90.
- (70) Fletcher, R. A new approach to variable metric algorithms. *Comput. J.* **1970**, *13*, 317–322.
- (71) Goldfarb, D. A family of variable-metric methods derived by variational means. *Math. Comput.* **1970**, *24*, 23–26.
- (72) Shanno, D. F. Conditioning of quasi-Newton methods for function minimization. *Math. Comput.* **1970**, *24*, 647–656.
- (73) Hastings, M. B.; Wecker, D.; Bauer, B.; Troyer, M. Improving Quantum Algorithms for Quantum Chemistry. *Quantum Info. Comput.* **2015**, *15*, 1–21.
- (74) Knowles, P. J.; Handy, N. C. A new determinant-based full configuration interaction method. *Chem. Phys. Lett.* **1984**, *111*, 315–321.
- (75) Lee, J.; Huggins, W. J.; Head-Gordon, M.; Whaley, K. B. Generalized unitary coupled cluster wave functions for quantum computation. *J. Chem. Theory Comput.* **2018**, *15*, 311–324.
- (76) Foss-Feig, M.; Hayes, D.; Dreiling, J. M.; Figgatt, C.; Gaebler, J. P.; Moses, S. A.; Pino, J. M.; Potter, A. C. Holographic quantum algorithms for simulating correlated spin systems. *Phys. Rev. Res.* **2021**, *3*, 033002.
- (77) Haghshenas, R.; Gray, J.; Potter, A. C.; Chan, G. K. The Variational Power of Quantum Circuit Tensor Networks. *arXiv preprint arXiv:2107.01307* **2021**,
- (78) Seki, K.; Yunoki, S. Quantum power method by a superposition of time-evolved states. *Phys. Rev. X Quantum* **2021**, *2*, 010333.
- (79) Ollitrault, P. J.; Kandala, A.; Chen, C.-F.; Barkoutsos, P. K.; Mezzacapo, A.; Pistoia, M.; Sheldon, S.; Woerner, S.; Gambetta, J. M.; Tavernelli, I. Quantum equation of motion for computing molecular excitation energies on a noisy quantum processor. *Phys. Rev. Res.* **2020**, *2*, 043140.
- (80) Bravyi, S.; Gambetta, J. M.; Mezzacapo, A.; Temme, K. Tapering off qubits to simulate fermionic Hamiltonians. *arXiv preprint arXiv:1701.08213* **2017**,
- (81) Huggins, W. J.; McClean, J. R.; Rubin, N. C.; Jiang, Z.; Wiebe, N.; Whaley, K. B.; Babbush, R. Efficient and noise resilient measurements for quantum chemistry on near-term quantum computers. *npj Quantum Inf.* **2021**, *7*, 1–9.